Dynamical singularities in adaptive delayed-feedback control

Asaki Saito[1,2,*] and Keiji Konishi[3]

[1]*Future University Hakodate, 116-2 Kameda Nakano-cho, Hakodate, Hokkaido 041-8655, Japan*

[2]*PRESTO, Japan Science and Technology Agency, 4-1-8 Honcho, Kawaguchi, Saitama 332-0012, Japan*

[3]*Osaka Prefecture University, 1-1 Gakuen-cho, Sakai, Osaka 599-8531, Japan*

(Received 15 January 2011; published 1 September 2011)

We demonstrate the dynamical characteristics of adaptive delayed-feedback control systems, exploiting a discrete-time adaptive control method derived for carrying out detailed analysis. In particular, the systems exhibit singularities such as power-law decay of the distribution of transient times and almost zero finite-time Lyapunov exponents. We can explain these results by characterizing such systems as having (1) a Jacobian matrix with unity eigenvalue in the whole phase space, and (2) parameters approaching a stability boundary proven to be identical with that of (nonadaptive) delayed-feedback control.

DOI: 10.1103/PhysRevE.84.031902 PACS number(s): 87.10.−e, 05.45.Gg, 89.75.−k

I. INTRODUCTION

The ability to adapt, as by learning, is indispensable for the survival of living things, and can also be critical in other real systems, e.g., ecological, economic, and social systems. Extensive studies relating to the realization of such ability in artificial systems have been carried out in diverse fields, including physics. Neural networks have attracted particular attention from physicists. Although these studies have achieved significant success, some intractable aspects of such adaptive systems as dynamical systems have also been reported. Not just real biological systems, but even much simpler, artificially constructed systems often exhibit highly dynamic and complex behavior (see Refs. [1–3]); for example, we have previously identified singular behavior ("neutral behavior") different from ordinary chaos, such as that exemplified by zero Lyapunov exponents [4]. To understand highly dynamic phenomena, e.g., of living things, it is necessary to analyze the complex dynamics of such adaptive processes themselves, in contrast to conventional treatments, which tend to focus on efficiency or stability. However, relatively few such analyses have been done so far, and these studies have been limited to reports of individual phenomena observed numerically. This is in part because an adaptive system itself, as well as its dynamics, tends to be extraordinarily complex and thus difficult to analyze, as reported previously for online learning of recurrent neural networks [4]. In this paper, we study, not merely numerically but also theoretically, a much simpler but sufficiently general class of adaptive systems derived from controlling chaos. That is, we study dynamical system characteristics of adaptive delayed-feedback control, employing an adaptive control method developed for performing rigorous analysis.

Delayed-feedback control (DFC) [5] is one of the two standard methods for controlling chaos, allowing the stabilization of an unstable periodic orbit. DFC can be used without knowledge of the target orbits, in contrast to the other standard method, proposed by Ott, Grebogi, and Yorke (the OGY method) [6]. Since both methods are deterministic, a control system (i.e., a total system where a dynamical system is controlled by such a method) also becomes a dynamical system. To carry out detailed analysis, we use DFC as the basis of our study because of its remarkable simplicity. Indeed, this method can produce much simpler dynamical systems as control systems than the OGY method because DFC systems do not require reference signals, i.e., external inputs for specifying target orbits. For the purpose of clarifying the dynamical features of adaptive processes, we derived a discrete-time adaptive DFC method where the DFC is expanded into adaptive control. Even with this modification, our adaptive DFC is still far simpler, and thus far easier to analyze, than the previously studied online learning of recurrent neural networks [4]. However, even for (nonadaptive) DFC, few investigations of the global dynamics of control systems exist, except, e.g., Refs. [7,8], although their local properties have been studied intensively [9–11].

In this paper, in order to clarify characteristics of adaptive processes as dynamical system processes, we investigate both the local and global properties of adaptive DFC systems by linear stability analysis and numerical simulations using the Hénon map. As a result, we show that the dynamics of adaptive DFC systems are indeed singular ("neutral"), in strong contrast to ordinary chaos, and, in particular, that this singularity is well explained by two distinct characteristics, local and global, demonstrated for adaptive DFC systems.

II. ADAPTIVE DELAYED-FEEDBACK CONTROL

While DFC was originally proposed as a method for controlling chaos in continuous-time dynamical systems [5], it can also be applied to discrete-time systems [12,13] such as $\mathbf{x}(t+1) = \boldsymbol{f}(\mathbf{x}(t)) + \mathbf{K}[\mathbf{x}(t-T) - \mathbf{x}(t)]$, where $\mathbf{x}(t) \in \mathbb{R}^n$ is a state at discrete times $t = 0,1,2,\ldots$, $\boldsymbol{f}$ is an n-dimensional map to be controlled, $\mathbf{K}$ is an $n \times n$ constant matrix called a gain matrix, and T is the period of an unstable periodic orbit of $\boldsymbol{f}$ to be stabilized. If we can determine an appropriate $\mathbf{K}$, unstable periodic orbits with period T will be stabilized. However, such a determination is generally difficult [13,14]. Thus, we require an adaptive control method that automatically adjusts parameters, such as elements of $\mathbf{K}$. As far as we know, no adaptive DFC method has previously been proposed for discrete-time systems, while there are several for continuous-time systems. In order to simplify the following analysis, next we derive a discrete-time adaptive DFC method, which is a discrete-time version of the continuous-time adaptive DFC method proposed by Nakajima *et al.* [15].

*saito@fun.ac.jp

In the following, we focus on the stabilization of unstable fixed points ($T = 1$)

$$\mathbf{x}(t+1) = \boldsymbol{f}(\mathbf{x}(t)) + \mathbf{K}(t)[\mathbf{x}(t-1) - \mathbf{x}(t)] \tag{1}$$

because stabilization of period-T orbits of $\boldsymbol{f}$ can be reduced to that of fixed points of the T-times composed map $\boldsymbol{f}^{(T)}$. The update of $\mathbf{K}$ is based on a gradient descent of the squared error $E(t) = \frac{1}{2}\|\mathbf{x}(t-1) - \mathbf{x}(t)\|^2$, where E implicitly depends on $\mathbf{K}$ through $\mathbf{x}$. Suppose the (i,j)th element k_{ij} of $\mathbf{K}$ is one of the adjustable parameters; the update rule for k_{ij} is given by

$$\begin{aligned} k_{ij}(t+1) &= k_{ij}(t) - \varepsilon \left.\frac{\partial E(t)}{\partial k_{ij}}\right|_{\mathbf{K}(t)} \\ &= k_{ij}(t) - \varepsilon[\mathbf{x}(t-1) - \mathbf{x}(t)] \cdot [\mathbf{v}_{ij}(t-1) - \mathbf{v}_{ij}(t)], \end{aligned} \tag{2}$$

where $\varepsilon > 0$ denotes a learning rate and $\mathbf{v}_{ij}(t)$ denotes $\frac{\partial \mathbf{x}(t)}{\partial k_{ij}}$. By assuming that $\mathbf{K}$ is constant in time, the approximate equation for $\mathbf{v}_{ij}(t)$ is derived from differentiating Eq. (1) by k_{ij}, yielding

$$\begin{aligned} \mathbf{v}_{ij}(t+1) = {} & \mathbf{D}\boldsymbol{f}(\mathbf{x}(t))\mathbf{v}_{ij}(t) + \mathbf{K}(t)[\mathbf{v}_{ij}(t-1) - \mathbf{v}_{ij}(t)] \\ & + [x_j(t-1) - x_j(t)]\mathbf{e}_i, \end{aligned} \tag{3}$$

where $\mathbf{D}\boldsymbol{f}(\mathbf{x})$ is a Jacobian matrix of $\boldsymbol{f}$ at $\mathbf{x}$, x_j is the jth element of $\mathbf{x}$, and $\mathbf{e}_i$ is the ith unit vector.[1] We now accomplish the derivation of the discrete-time adaptive DFC method by Eqs. (1)–(3).[2]

For simplicity, we arrange all the parameters (i.e., the adjustable elements of $\mathbf{K}$) as a d-dimensional vector $\boldsymbol{\kappa}$, where d is the number of the parameters. Equations (1)–(3) then constitute a dynamical system with delay, with dynamical variables $\{\mathbf{x}(t), \kappa_l(t), \mathbf{v}_l(t)\}$ $(l = 1,2,\ldots,d)$, where κ_l is the lth element of the $\boldsymbol{\kappa}$ and $\mathbf{v}_l(t)$ is $\frac{\partial \mathbf{x}(t)}{\partial \kappa_l}$. This dynamical system with delay can be rewritten as a dynamical system without delay by introducing new variables $\mathbf{y}(t)$ and $\mathbf{w}_l(t)$ for $\mathbf{x}(t-1)$ and $\mathbf{v}_l(t-1)$, respectively, as follows:

$$\begin{aligned} \mathbf{x}(t+1) &= \boldsymbol{f}(\mathbf{x}(t)) + \mathbf{K}(t)[\mathbf{y}(t) - \mathbf{x}(t)], \\ \mathbf{y}(t+1) &= \mathbf{x}(t), \\ \kappa_l(t+1) &= \kappa_l(t) - \varepsilon[\mathbf{y}(t) - \mathbf{x}(t)] \cdot [\mathbf{w}_l(t) - \mathbf{v}_l(t)], \\ \mathbf{v}_l(t+1) &= \mathbf{D}\boldsymbol{f}(\mathbf{x}(t))\mathbf{v}_l(t) + \mathbf{K}(t)[\mathbf{w}_l(t) - \mathbf{v}_l(t)] \\ &\quad + [y_{j(l)}(t) - x_{j(l)}(t)]\mathbf{e}_{i(l)}, \\ \mathbf{w}_l(t+1) &= \mathbf{v}_l(t), \end{aligned} \tag{4}$$

where $l = 1,2,\ldots,d$. Also, $i(l)$ represents the row index and $j(l)$ the column index of k_{ij}, which corresponds to κ_l. We call this dynamical system an adaptive DFC system.

III. LINEAR STABILITY ANALYSIS

In this section, we demonstrate the *local properties* of adaptive DFC systems by using linear stability analysis. We state below three facts (Facts 1–3); a detailed description of the Jacobian matrix of the adaptive DFC systems [Eq. (4)], which is necessary to prove Facts 1 and 3, is provided in Appendix A.

First, we demonstrate the uniqueness of the adaptive DFC systems as dynamical systems by showing the distinctive feature of the Jacobian matrix of Eq. (4).

Fact 1 The Jacobian matrix of the adaptive DFC systems [Eq. (4)] has eigenvalue unity at all points in phase space, except for points where the matrix is not defined.

A proof of Fact 1 is presented in Appendix B. For discrete-time dynamical systems, the eigenvalue unity of the Jacobian matrix at some point indicates the existence of one-step neutral stability of dynamics around that point. Fact 1 reveals that the adaptive DFC systems have such neutral stability over the entire phase space, which is a unique situation compared to other dynamical systems. As will be shown in the next section, we also observe unique behavior in adaptive DFC processes numerically: The behavior is neutral behavior different from ordinary chaos, such as power-law decay of the distribution of transient times and almost zero finite-time Lyapunov exponents. The local characteristic stated in Fact 1 can allow us to understand why adaptive DFC systems so widely exhibit such neutral behavior.[3]

While Fact 1 holds true throughout the whole phase space, we can conduct further analysis on the adaptive DFC systems, in particular around fixed points. In fact, we can prove the following two facts, for the fixed points of Eq. (4):

Fact 2 Let $\mathbf{x}_*$ be a fixed point of $\boldsymbol{f}$, and let $\mathbf{z}_1, \mathbf{z}_2, \ldots, \mathbf{z}_d$ be eigenvectors associated with the eigenvalue unity of $\mathbf{D}\boldsymbol{f}(\mathbf{x}_*)$. Then every fixed point of Eq. (4) takes the form $(\mathbf{x}, \mathbf{y}, \kappa_1, \kappa_2, \ldots, \kappa_d, \mathbf{v}_1, \mathbf{w}_1, \mathbf{v}_2, \mathbf{w}_2, \ldots, \mathbf{v}_d, \mathbf{w}_d) = (\mathbf{x}_*, \mathbf{x}_*, c_1, c_2, \ldots, c_d, \mathbf{z}_1, \mathbf{z}_1, \mathbf{z}_2, \mathbf{z}_2, \ldots, \mathbf{z}_d, \mathbf{z}_d)$, where $c_1, c_2, \ldots, c_d$ are constants. If $\mathbf{D}\boldsymbol{f}(\mathbf{x}_*)$ does not have the eigenvalue unity, then $\mathbf{z}_1, \mathbf{z}_2, \ldots, \mathbf{z}_d$ are all $\mathbf{0}$.

See Appendix C for the derivation of the fixed points of Eq. (4).

Since our control task is to stabilize a fixed point, we require the state of the adaptive DFC systems themselves to converge to a fixed point, after the control ends in success. Conversely, Fact 2 reveals that all fixed points of Eq. (4) are successful states because the $\mathbf{x}$ component, corresponding to the original variable of the undelayed system, equals the original fixed point $\mathbf{x}_*$. In the case of the adaptive DFC, therefore, we can identify success of control with convergence to a fixed point, and the stability of the fixed points becomes a matter of concern.

[1] The initial value for $\mathbf{v}_{ij}$ is given by $\mathbf{v}_{ij}(0) = \mathbf{v}_{ij}(-1) = \mathbf{0}$.

[2] This online update scheme is the same as that used in the continuous-time adaptive DFC and the online learning of recurrent neural networks, and has been successfully applied to various temporal adaptation tasks [15–17].

[3] As far as we know, at least for dynamical systems that we usually encounter, power-law decay of the distribution of transient times implies existence of a finite-time Lyapunov exponent around zero (the exponent is not necessarily the largest one, and possibly exhibits irregular oscillation around zero [4]). Several mechanisms are well known to generate such neutral behavior; for example, various intermittency mechanisms at a critical point [18]. In contrast, for a given dynamical system exhibiting neutral behavior, it is still difficult in general to identify the mechanism explaining the observed neutral behavior. In Sec. IV D, we provide another reason (a global reason) for the neutral behavior observed in adaptive DFC processes.

Fact 3 Consider the map for nonadaptive DFC systems

$$\begin{aligned}\mathbf{x}(t+1) &= \boldsymbol{f}(\mathbf{x}(t)) + \mathbf{K}[\mathbf{y}(t) - \mathbf{x}(t)],\\ \mathbf{y}(t+1) &= \mathbf{x}(t),\end{aligned} \tag{5}$$

which has a fixed point $(\mathbf{x},\mathbf{y}) = (\mathbf{x}_*,\mathbf{x}_*)$. Let $\Phi(\lambda)$ be the characteristic polynomial of the Jacobian matrix of Eq. (5) at the fixed point. Then, the characteristic equation of the Jacobian matrix of Eq. (4) at the fixed points described in Fact 2 is given by

$$(\lambda - 1)^d[\Phi(\lambda)]^{d+1} = 0. \tag{6}$$

A proof of Fact 3 is presented in Appendix D.

In particular, Fact 3 reveals that the stability condition for the fixed points of the adaptive DFC is identical with that of the nonadaptive DFC, except for the eigenvalue unity, from the factor $(\lambda - 1)^d$ in Eq. (6).[4] Later, we will exploit this identity to provide another reason (a global reason) for the neutral behavior that we now move on to consider.

IV. NUMERICAL SIMULATIONS

In the following, we explore the *global properties* of the adaptive DFC systems by numerical simulations.[5] As a typical example, we present results obtained using the Hénon map $(x_1,x_2) \mapsto (a - x_1^2 + bx_2,x_1)$ with parameter values $(a,b) = (1.4,0.3)$, although similar results have been obtained in other cases using different parameters or different chaotic maps (e.g., the logistic, tent, and Lozi maps).

A. Basin structure

First, we study the basin structure of adaptive DFC systems. Figures 1(a) and 1(b) show a two-dimensional slice through initial condition space using adaptive and nonadaptive DFC, respectively, for stabilization of an unstable fixed point $\mathbf{x}_*$ of the Hénon map.[6] The horizontal and vertical axes correspond to $y_1(0)$ and $y_2(0)$, respectively. The other initial values are $\mathbf{x}(0) = \boldsymbol{f}(\mathbf{y}(0))$ and $\mathbf{K}(0) = \left(\begin{smallmatrix}-0.8 & 0\\ 0 & 0\end{smallmatrix}\right)$ (cf. footnote 1). For the adaptive control, we choose to update all four elements of $\mathbf{K}$ as adjustable parameters, with $\varepsilon = 0.0001$. In this setting, the adaptive DFC system is a 24-dimensional map from Eq. (4), whereas the map for the nonadaptive DFC is 4 dimensional from Eq. (5). In either figure, each initial condition on a $10^3 \times 10^3$ grid is followed until 10^5 time steps. Grid points are plotted as black dots for initial conditions from which control ends in success (i.e., from which control achieves convergence to $\mathbf{x}_*$); otherwise, points are left blank. These figures show fine

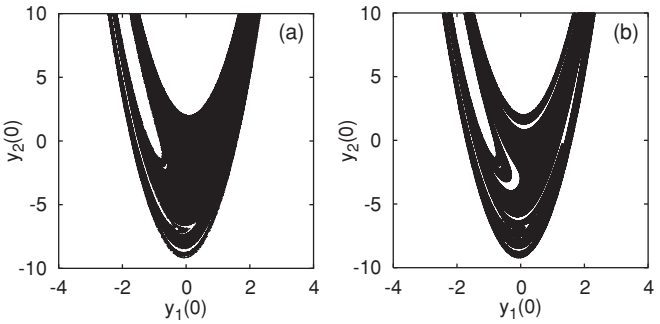

FIG. 1. Initial conditions with success, plotted as black dots, for (a) adaptive DFC and (b) nonadaptive DFC.

structure, which implies sensitivity to the initial conditions of whether control results in success. Furthermore, the basin volume (area) shown in Fig. 1(a) increases over that in Fig. 1(b) by 14.1%, indicating the superior efficiency of our discrete-time adaptive DFC method.

B. Distribution of control times

Next, we shift our focus to the construction process of such fractal basins. In particular, we study the distribution of control times (transient times). Figures 2(a) and 2(b) show control time distribution of adaptive and nonadaptive DFC, respectively. In each case, $\mathbf{y}(0)$ is uniformly chosen from a bounded region (the region $[-2,2] \times [-2,2]$). The other settings are the same as the basin's case before. As a result, in the case of the adaptive DFC, a fraction of the initial points from which control ends in success with control time τ, denoted as $p(\tau)$, is found to decay according to a power law. This "slow" decay is in strong contrast with "fast" decay observed in transient chaos: In general, distribution of transient times decays exponentially for transient chaos (i.e., construction process of ordinary fractals) [19]. Indeed, $p(\tau)$ decays exponentially in nonadaptive DFC.

C. Time evolution

The slow decay indicates the existence of underlying long transients. To clarify the underlying dynamics of the observed power-law distribution [Fig. 2(a)], we further give results on the time evolution of long-transient orbits of adaptive DFC systems using a finite-time Lyapunov exponent. The time-t Lyapunov exponent is the average exponential expansion rate along the trajectory of length t [19]. In this paper, we focus on the largest exponent. Figure 3(a) presents $x_1(t)$ versus t

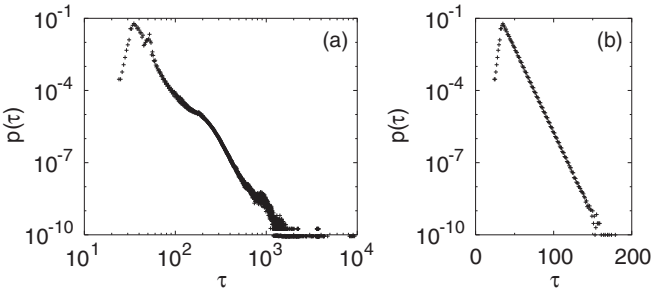

FIG. 2. Distributions of control times for (a) adaptive DFC (log-log plot) and (b) nonadaptive DFC (semilog plot).

[4]Note that Fact 3 holds true only for the fixed points, whereas Fact 1 holds true throughout the whole phase space, including the fixed points.

[5]While we have examined the adaptive DFC only through numerical simulations, it can be applied to various physical systems, as can the nonadaptive DFC.

[6]In fact, the Hénon map with $(a,b) = (1.4,0.3)$ has two unstable fixed points. However, because of the odd number limitation [13], DFC can stabilize only one of them, i.e., the fixed point $\mathbf{x}_* = (\alpha,\alpha)^{\mathrm{T}}$, where $\alpha = \frac{1}{2}\{b - 1 + [(b-1)^2 + 4a]^{1/2}\} \approx 0.883\,896\ldots$.

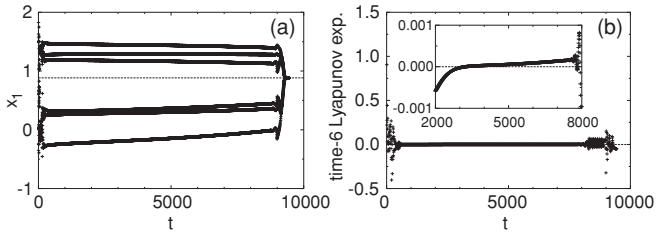

FIG. 3. Time evolution for the adaptive DFC. (a) $x_1(t)$ vs t. The dashed line for the position of the x_1 component of $\mathbf{x}_*$ (cf. footnote 6). (b) The time-6 Lyapunov exponent vs t. Inset: A magnification for $2000 \leqslant t \leqslant 8000$.

of an orbit starting from the initial condition $[y_1(0), y_2(0)] \approx (-1.350\,32, 0.609\,88)$, which is chosen to generate a long-transient orbit from the data of Fig. 2(a). In this example, the orbit has a transient of nearly 10^4 time steps, and shows period-6 motion in most of the transient time, but the control results in success. Figure 3(b) shows the time-6 Lyapunov exponent versus t, with the same conditions as in Fig. 3(a). As a result, the finite-time Lyapunov exponent is almost 0. However, more precisely, its value changes sign from slightly negative to slightly positive [inset in Fig. 3(b)], indicating a corresponding slight change of the stability of the pseudo-period-6 orbit. Similar dynamical behavior dominated by periodic or quasiperiodic motion with almost zero finite-time Lyapunov exponents is typically observed for other long-transient orbits, independently of other choices of initial values, parameter values, arrangement of adjustable elements in $\mathbf{K}$, and controlled chaotic maps.

D. Dynamics in parameter space

The above observations indicate that the dynamics of adaptive DFC systems are neutral in the sense that (i) transient time (control time) distribution decays according to a power law and (ii) the finite-time Lyapunov exponent is almost 0. In the following, we investigate dynamics in parameter space and give another reason why such neutral behavior is observed in adaptive DFC processes, from the viewpoint of global dynamics.

To demonstrate parameter dynamics, we use only two elements, k_{11} and k_{12}, of $\mathbf{K}$ as adjustable parameters for the purpose of visibility. In this case, we obtain a 14-dimensional map from Eq. (4). The other settings are the same as before. In Fig. 4, trajectories in parameter space are displayed for several orbits with long transients. All of these start from the same initial parameters $[k_{11}(0), k_{12}(0)] = (-0.8, 0)$ but from different $\mathbf{y}(0)$, indicated by different colors (gray levels). In this case, one can verify, by using the Jury criterion [20], that the fixed point $(\mathbf{x}_*, \mathbf{x}_*)$ of the nonadaptive DFC system [Eq. (5)] is locally stable if and only if k_{11} and k_{12} satisfy the following inequalities:

$$\frac{-k_{12}^2 - (2\alpha+1)k_{12} + b + 1}{k_{12} - 1} < k_{11} < k_{12} - \frac{2\alpha + b - 1}{2}, \qquad -1 < k_{12} < 1 \tag{7}$$

where $\alpha \approx 0.883\,896\ldots$ and $b = 0.3$. The closed curve in Fig. 4 shows the boundary of this stability region. As a

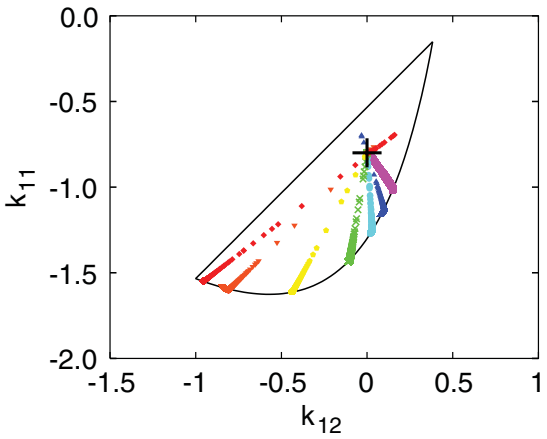

FIG. 4. (Color online) Trajectories in parameter space for two-parameter adaptive DFC. All the trajectories originate from $[k_{11}(0), k_{12}(0)] = (-0.8, 0)$ labeled as the plus sign. Different colors (gray levels) indicate different initial conditions. The closed curve represents the stability boundary given by Eq. (7).

result, the parameters (k_{11}, k_{12}) of all the long-transient orbits approach and stay near the boundary, where the fixed point of Eq. (5) is neutrally stable, and, accordingly, Φ in Eq. (6) itself has a root of modulus unity. Similar approaches of parameters to a stability boundary have been widely observed for other adaptive DFC systems with various different conditions. Thus, the neutral behaviors in the adaptive DFC systems can be also explained from the viewpoint of global dynamics, that is, approaches of parameters to a stability boundary. In general, various power-law distributions accompanied by zero Lyapunov exponents are observed at a critical point (see, e.g., Refs. [21–23]).

V. SUMMARY AND DISCUSSION

In this paper, in order to clarify dynamical features of adaptive processes, we have investigated adaptive DFC, both theoretically and numerically, by exploiting a discrete-time adaptive DFC method derived for carrying out detailed analysis. In particular, we demonstrated that, as dynamical systems, adaptive DFC systems exhibit singular behavior ("neutral behavior") different from ordinary chaos. Furthermore, we have shown that these singularities can be explained by the local characteristic that the Jacobian matrix has eigenvalue unity in the whole phase space, and by the global characteristic that parameters approach a stability boundary proven to be identical with that of the nonadaptive DFC.

It is our conjecture that unique dynamical singularities such as those reported here will be common in systems with the ability of adaptation or learning. Indeed, not only the numerical observation of similar singularity as mentioned already [4], but also a theoretical argument similar to this study can be made for the online learning of recurrent neural networks, which will be reported elsewhere. Further clarification of such universality will be crucial toward understanding highly dynamic and complex phenomena observed in real systems such as brains. (Indeed, a phenomenon resembling the present results, as well as a conjecture that parameters are near a stability boundary, has been reported in a study of human control of balance [24].)

ACKNOWLEDGMENTS

We thank S. Amari, I. Frank, T. Ikegami, S. Ito, K. Kaneko, M. Taiji, and I. Tsuda for their suggestions. This research was partly supported by a grant-in-aid from MEXT of Japan and by JST PRESTO program.

APPENDIX A: JACOBIAN MATRIX OF ADAPTIVE DFC SYSTEMS

In order to determine the Jacobian matrix of adaptive DFC systems [Eq. (4)], we first introduce several symbols. Let $\tilde{\mathbf{x}}$ be a state of the adaptive DFC systems given by

$$\tilde{\mathbf{x}} = (\mathbf{x},\mathbf{y},\boldsymbol{\kappa},\mathbf{v}_1,\mathbf{w}_1,\mathbf{v}_2,\mathbf{w}_2,\ldots,\mathbf{v}_d,\mathbf{w}_d),$$

and $\boldsymbol{F}$ be the map for the adaptive DFC systems. Then, Eq. (4) can be represented by

$$\tilde{\mathbf{x}}(t+1) = \boldsymbol{F}(\tilde{\mathbf{x}}(t)).$$

We denote the components of $\boldsymbol{F}$ by $\boldsymbol{F}_{\mathbf{x}},\boldsymbol{F}_{\mathbf{y}},\boldsymbol{F}_{\boldsymbol{\kappa}},\boldsymbol{F}_{\mathbf{v}_1},\boldsymbol{F}_{\mathbf{w}_1}$, $\boldsymbol{F}_{\mathbf{v}_2},\boldsymbol{F}_{\mathbf{w}_2},\ldots,\boldsymbol{F}_{\mathbf{v}_d},\boldsymbol{F}_{\mathbf{w}_d}$, which assign, respectively, the components $\mathbf{x},\mathbf{y},\boldsymbol{\kappa},\mathbf{v}_1,\mathbf{w}_1,\mathbf{v}_2,\mathbf{w}_2,\ldots,\mathbf{v}_d,\mathbf{w}_d$ of $\tilde{\mathbf{x}}$. That is,

$$\begin{aligned}
\mathbf{x}(t+1) &= \boldsymbol{F}_{\mathbf{x}}(\tilde{\mathbf{x}}(t)),\\
\mathbf{y}(t+1) &= \boldsymbol{F}_{\mathbf{y}}(\tilde{\mathbf{x}}(t)),\\
\boldsymbol{\kappa}(t+1) &= \boldsymbol{F}_{\boldsymbol{\kappa}}(\tilde{\mathbf{x}}(t)),\\
\mathbf{v}_1(t+1) &= \boldsymbol{F}_{\mathbf{v}_1}(\tilde{\mathbf{x}}(t)),\\
\mathbf{w}_1(t+1) &= \boldsymbol{F}_{\mathbf{w}_1}(\tilde{\mathbf{x}}(t)),\\
\mathbf{v}_2(t+1) &= \boldsymbol{F}_{\mathbf{v}_2}(\tilde{\mathbf{x}}(t)),\\
\mathbf{w}_2(t+1) &= \boldsymbol{F}_{\mathbf{w}_2}(\tilde{\mathbf{x}}(t)),\\
&\vdots\\
\mathbf{v}_d(t+1) &= \boldsymbol{F}_{\mathbf{v}_d}(\tilde{\mathbf{x}}(t)),\\
\mathbf{w}_d(t+1) &= \boldsymbol{F}_{\mathbf{w}_d}(\tilde{\mathbf{x}}(t)).
\end{aligned}$$

Also, we denote the $m \times m$ identity matrix by $\mathbf{I}_m$, and the $m \times n$ zero matrix, having only zero elements, by $\mathbf{0}_{m\times n}$.

In order to closely investigate the Jacobian matrix $\mathbf{D}\boldsymbol{F}$ of $\boldsymbol{F}$, we partition $\mathbf{D}\boldsymbol{F}$ as follows:

$$\mathbf{D}\boldsymbol{F}(\tilde{\mathbf{x}}) = \begin{matrix} \\ 2n+d \\ 2nd \end{matrix}\!\!\begin{matrix} \overbrace{\phantom{\mathbf{A}}}^{2n+d} & \overbrace{\phantom{\mathbf{B}}}^{2nd} \\ \left(\begin{matrix} \mathbf{A} & \mathbf{B} \\ \mathbf{C} & \mathbf{D} \end{matrix}\right), \end{matrix}$$

where $\mathbf{A}$, $\mathbf{B}$, $\mathbf{C}$, and $\mathbf{D}$ are $(2n+d)\times(2n+d)$, $(2n+d)\times 2nd$, $2nd\times(2n+d)$, and $2nd\times 2nd$ matrices, respectively. In the following, we carry out a determination of $\mathbf{D}\boldsymbol{F}$ through determination of each block in turn.

The block $\mathbf{A}$ of $\mathbf{D}\boldsymbol{F}$ is given by

$$\begin{aligned}
\mathbf{A} &= \begin{pmatrix} \partial\boldsymbol{F}_{\mathbf{x}}/\partial\mathbf{x} & \partial\boldsymbol{F}_{\mathbf{x}}/\partial\mathbf{y} & \partial\boldsymbol{F}_{\mathbf{x}}/\partial\boldsymbol{\kappa} \\ \partial\boldsymbol{F}_{\mathbf{y}}/\partial\mathbf{x} & \partial\boldsymbol{F}_{\mathbf{y}}/\partial\mathbf{y} & \partial\boldsymbol{F}_{\mathbf{y}}/\partial\boldsymbol{\kappa} \\ \partial\boldsymbol{F}_{\boldsymbol{\kappa}}/\partial\mathbf{x} & \partial\boldsymbol{F}_{\boldsymbol{\kappa}}/\partial\mathbf{y} & \partial\boldsymbol{F}_{\boldsymbol{\kappa}}/\partial\boldsymbol{\kappa} \end{pmatrix} \\
&= \begin{pmatrix} \mathbf{D}\boldsymbol{f}-\mathbf{K} & \mathbf{K} & \mathbf{A}_{1,3} \\ \mathbf{I}_n & \mathbf{0}_{n\times n} & \mathbf{0}_{n\times d} \\ \mathbf{A}_{3,1} & \mathbf{A}_{3,2} & \mathbf{I}_d \end{pmatrix}. \qquad \text{(A1)}
\end{aligned}$$

$\mathbf{A}_{1,3}$ is a $n\times d$ matrix with the $[i(l),l]$th element $y_{j(l)}-x_{j(l)}$ for $l=1,2,\ldots,d$, while the other elements are equal to zero. [Note again that $i(l)$ represents the row index and $j(l)$ the column index of k_{ij}, which corresponds to κ_l.] The $d\times n$ matrices $\mathbf{A}_{3,1}$ and $\mathbf{A}_{3,2}$ are given by

$$\mathbf{A}_{3,1} = \begin{pmatrix} \varepsilon(\mathbf{w}_1-\mathbf{v}_1)^{\mathrm{T}} \\ \varepsilon(\mathbf{w}_2-\mathbf{v}_2)^{\mathrm{T}} \\ \vdots \\ \varepsilon(\mathbf{w}_d-\mathbf{v}_d)^{\mathrm{T}} \end{pmatrix}, \quad \mathbf{A}_{3,2} = \begin{pmatrix} -\varepsilon(\mathbf{w}_1-\mathbf{v}_1)^{\mathrm{T}} \\ -\varepsilon(\mathbf{w}_2-\mathbf{v}_2)^{\mathrm{T}} \\ \vdots \\ -\varepsilon(\mathbf{w}_d-\mathbf{v}_d)^{\mathrm{T}} \end{pmatrix},$$

where the superscript T denotes transpose.

The block $\mathbf{B}$ of $\mathbf{D}\boldsymbol{F}$ is given by

$$\begin{aligned}
\mathbf{B} &= \begin{pmatrix} \partial\boldsymbol{F}_{\mathbf{x}}/\partial\mathbf{v}_1 & \partial\boldsymbol{F}_{\mathbf{x}}/\partial\mathbf{w}_1 & \ldots & \partial\boldsymbol{F}_{\mathbf{x}}/\partial\mathbf{v}_d & \partial\boldsymbol{F}_{\mathbf{x}}/\partial\mathbf{w}_d \\ \partial\boldsymbol{F}_{\mathbf{y}}/\partial\mathbf{v}_1 & \partial\boldsymbol{F}_{\mathbf{y}}/\partial\mathbf{w}_1 & \ldots & \partial\boldsymbol{F}_{\mathbf{y}}/\partial\mathbf{v}_d & \partial\boldsymbol{F}_{\mathbf{y}}/\partial\mathbf{w}_d \\ \partial\boldsymbol{F}_{\boldsymbol{\kappa}}/\partial\mathbf{v}_1 & \partial\boldsymbol{F}_{\boldsymbol{\kappa}}/\partial\mathbf{w}_1 & \ldots & \partial\boldsymbol{F}_{\boldsymbol{\kappa}}/\partial\mathbf{v}_d & \partial\boldsymbol{F}_{\boldsymbol{\kappa}}/\partial\mathbf{w}_d \end{pmatrix} \\
&= \begin{pmatrix} \mathbf{0}_{n\times n} & \mathbf{0}_{n\times n} & \ldots & \mathbf{0}_{n\times n} & \mathbf{0}_{n\times n} \\ \mathbf{0}_{n\times n} & \mathbf{0}_{n\times n} & \ldots & \mathbf{0}_{n\times n} & \mathbf{0}_{n\times n} \\ \mathbf{B}_{3,1} & \mathbf{B}_{3,2} & \ldots & \mathbf{B}_{3,2d-1} & \mathbf{B}_{3,2d} \end{pmatrix}. \qquad \text{(A2)}
\end{aligned}$$

$\mathbf{B}_{3,2l-1} = \partial\boldsymbol{F}_{\boldsymbol{\kappa}}/\partial\mathbf{v}_l$ and $\mathbf{B}_{3,2l} = \partial\boldsymbol{F}_{\boldsymbol{\kappa}}/\partial\mathbf{w}_l$ $(l=1,2,\ldots,d)$ are $d\times n$ matrices, where the lth rows are $\varepsilon(\mathbf{y}-\mathbf{x})^{\mathrm{T}}$ and $-\varepsilon(\mathbf{y}-\mathbf{x})^{\mathrm{T}}$, respectively. All other elements are equal to zero. Thus, the forms of $\mathbf{B}_{3,2l-1}$ and $\mathbf{B}_{3,2l}$ are as follows:

$$\mathbf{B}_{3,2l-1} = \begin{pmatrix} \mathbf{0}_{(l-1)\times n} \\ \varepsilon(\mathbf{y}-\mathbf{x})^{\mathrm{T}} \\ \mathbf{0}_{(d-l)\times n} \end{pmatrix}, \quad \mathbf{B}_{3,2l} = \begin{pmatrix} \mathbf{0}_{(l-1)\times n} \\ -\varepsilon(\mathbf{y}-\mathbf{x})^{\mathrm{T}} \\ \mathbf{0}_{(d-l)\times n} \end{pmatrix}.$$

The block $\mathbf{C}$ of $\mathbf{D}\boldsymbol{F}$ is given by

$$\begin{aligned}
\mathbf{C} &= \begin{pmatrix} \partial\boldsymbol{F}_{\mathbf{v}_1}/\partial\mathbf{x} & \partial\boldsymbol{F}_{\mathbf{v}_1}/\partial\mathbf{y} & \partial\boldsymbol{F}_{\mathbf{v}_1}/\partial\boldsymbol{\kappa} \\ \partial\boldsymbol{F}_{\mathbf{w}_1}/\partial\mathbf{x} & \partial\boldsymbol{F}_{\mathbf{w}_1}/\partial\mathbf{y} & \partial\boldsymbol{F}_{\mathbf{w}_1}/\partial\boldsymbol{\kappa} \\ \vdots & \vdots & \vdots \\ \partial\boldsymbol{F}_{\mathbf{v}_d}/\partial\mathbf{x} & \partial\boldsymbol{F}_{\mathbf{v}_d}/\partial\mathbf{y} & \partial\boldsymbol{F}_{\mathbf{v}_d}/\partial\boldsymbol{\kappa} \\ \partial\boldsymbol{F}_{\mathbf{w}_d}/\partial\mathbf{x} & \partial\boldsymbol{F}_{\mathbf{w}_d}/\partial\mathbf{y} & \partial\boldsymbol{F}_{\mathbf{w}_d}/\partial\boldsymbol{\kappa} \end{pmatrix} \\
&= \begin{pmatrix} \mathbf{C}_{1,1} & \mathbf{C}_{1,2} & \mathbf{C}_{1,3} \\ \mathbf{0}_{n\times n} & \mathbf{0}_{n\times n} & \mathbf{0}_{n\times d} \\ \vdots & \vdots & \vdots \\ \mathbf{C}_{2d-1,1} & \mathbf{C}_{2d-1,2} & \mathbf{C}_{2d-1,3} \\ \mathbf{0}_{n\times n} & \mathbf{0}_{n\times n} & \mathbf{0}_{n\times d} \end{pmatrix}. \qquad \text{(A3)}
\end{aligned}$$

The $n\times n$ matrices $\mathbf{C}_{2l-1,1}$ and $\mathbf{C}_{2l-1,2}$ and the $n\times d$ matrices $\mathbf{C}_{2l-1,3}$ $(l=1,2,\ldots,d)$ take somewhat complex forms. In particular, $\mathbf{C}_{2l-1,1}$ contains second derivatives of $\boldsymbol{f}$; this fact makes $\mathbf{D}\boldsymbol{F}$ be defined at points where $\boldsymbol{f}$ in Eq. (4) is twice differentiable. However, as long as $\mathbf{D}\boldsymbol{F}$ is defined, the contents of $\mathbf{C}_{2l-1,1}$, $\mathbf{C}_{2l-1,2}$, $\mathbf{C}_{2l-1,3}$ are unrelated to the presented discussion concerning Facts 1 and 3.

The block $\mathbf{D}$ of $\mathbf{D}\boldsymbol{F}$ has a block diagonal structure given by

$$\mathbf{D} = \begin{pmatrix} \partial \boldsymbol{F}_{\mathbf{v}_1}/\partial \mathbf{v}_1 & \partial \boldsymbol{F}_{\mathbf{v}_1}/\partial \mathbf{w}_1 & \dots & \partial \boldsymbol{F}_{\mathbf{v}_1}/\partial \mathbf{v}_d & \partial \boldsymbol{F}_{\mathbf{v}_1}/\partial \mathbf{w}_d \\ \partial \boldsymbol{F}_{\mathbf{w}_1}/\partial \mathbf{v}_1 & \partial \boldsymbol{F}_{\mathbf{w}_1}/\partial \mathbf{w}_1 & \dots & \partial \boldsymbol{F}_{\mathbf{w}_1}/\partial \mathbf{v}_d & \partial \boldsymbol{F}_{\mathbf{w}_1}/\partial \mathbf{w}_d \\ \vdots & \vdots & \ddots & \vdots & \vdots \\ \partial \boldsymbol{F}_{\mathbf{v}_d}/\partial \mathbf{v}_1 & \partial \boldsymbol{F}_{\mathbf{v}_d}/\partial \mathbf{w}_1 & \dots & \partial \boldsymbol{F}_{\mathbf{v}_d}/\partial \mathbf{v}_d & \partial \boldsymbol{F}_{\mathbf{v}_d}/\partial \mathbf{w}_d \\ \partial \boldsymbol{F}_{\mathbf{w}_d}/\partial \mathbf{v}_1 & \partial \boldsymbol{F}_{\mathbf{w}_d}/\partial \mathbf{w}_1 & \dots & \partial \boldsymbol{F}_{\mathbf{w}_d}/\partial \mathbf{v}_d & \partial \boldsymbol{F}_{\mathbf{w}_d}/\partial \mathbf{w}_d \end{pmatrix} = \begin{pmatrix} \mathbf{D}f - \mathbf{K} & \mathbf{K} & & & \mathbf{O} \\ \mathbf{I}_n & \mathbf{0}_{n\times n} & & & \\ & & \ddots & & \\ & & & \mathbf{D}f - \mathbf{K} & \mathbf{K} \\ \mathbf{O} & & & \mathbf{I}_n & \mathbf{0}_{n\times n} \end{pmatrix}. \tag{A4}$$

That is,

$$\begin{pmatrix} \partial \boldsymbol{F}_{\mathbf{v}_l}/\partial \mathbf{v}_l & \partial \boldsymbol{F}_{\mathbf{v}_l}/\partial \mathbf{w}_l \\ \partial \boldsymbol{F}_{\mathbf{w}_l}/\partial \mathbf{v}_l & \partial \boldsymbol{F}_{\mathbf{w}_l}/\partial \mathbf{w}_l \end{pmatrix} = \begin{pmatrix} \mathbf{D}f - \mathbf{K} & \mathbf{K} \\ \mathbf{I}_n & \mathbf{0}_{n\times n} \end{pmatrix}$$

for $l = 1,2,\dots,d$, and the other derivatives are equal to zero.

From Eqs. (A1)–(A4), we obtain the form of $\mathbf{D}\boldsymbol{F}$ as follows:

$$\mathbf{D}\boldsymbol{F} = \begin{pmatrix} \mathbf{D}f - \mathbf{K} & \mathbf{K} & \mathbf{A}_{1,3} & \mathbf{0}_{n\times n} & \mathbf{0}_{n\times n} & \dots & \mathbf{0}_{n\times n} & \mathbf{0}_{n\times n} \\ \mathbf{I}_n & \mathbf{0}_{n\times n} & \mathbf{0}_{n\times d} & \mathbf{0}_{n\times n} & \mathbf{0}_{n\times n} & \dots & \mathbf{0}_{n\times n} & \mathbf{0}_{n\times n} \\ \mathbf{A}_{3,1} & \mathbf{A}_{3,2} & \mathbf{I}_d & \mathbf{B}_{3,1} & \mathbf{B}_{3,2} & \dots & \mathbf{B}_{3,2d-1} & \mathbf{B}_{3,2d} \\ \mathbf{C}_{1,1} & \mathbf{C}_{1,2} & \mathbf{C}_{1,3} & \mathbf{D}f - \mathbf{K} & \mathbf{K} & & & \mathbf{O} \\ \mathbf{0}_{n\times n} & \mathbf{0}_{n\times n} & \mathbf{0}_{n\times d} & \mathbf{I}_n & \mathbf{0}_{n\times n} & & & \\ \vdots & \vdots & \vdots & & & \ddots & & \\ \mathbf{C}_{2d-1,1} & \mathbf{C}_{2d-1,2} & \mathbf{C}_{2d-1,3} & & & & \mathbf{D}f - \mathbf{K} & \mathbf{K} \\ \mathbf{0}_{n\times n} & \mathbf{0}_{n\times n} & \mathbf{0}_{n\times d} & \mathbf{O} & & & \mathbf{I}_n & \mathbf{0}_{n\times n} \end{pmatrix}. \tag{A5}$$

APPENDIX B: PROOF OF FACT 1

In order to prove Fact 1, we show that the determinant $|\mathbf{D}\boldsymbol{F} - \mathbf{I}_{2n+d+2nd}| = 0$ (see Appendix A for explanation of the symbols). From Eq. (A5),

$$|\mathbf{D}\boldsymbol{F} - \mathbf{I}_{2n+d+2nd}| = \begin{vmatrix} \mathbf{D}f - \mathbf{K} - \mathbf{I}_n & \mathbf{K} & \mathbf{A}_{1,3} & \mathbf{0}_{n\times n} & \mathbf{0}_{n\times n} & \dots & \mathbf{0}_{n\times n} & \mathbf{0}_{n\times n} \\ \mathbf{I}_n & -\mathbf{I}_n & \mathbf{0}_{n\times d} & \mathbf{0}_{n\times n} & \mathbf{0}_{n\times n} & \dots & \mathbf{0}_{n\times n} & \mathbf{0}_{n\times n} \\ \mathbf{A}_{3,1} & \mathbf{A}_{3,2} & \mathbf{0}_{d\times d} & \mathbf{B}_{3,1} & \mathbf{B}_{3,2} & \dots & \mathbf{B}_{3,2d-1} & \mathbf{B}_{3,2d} \\ \mathbf{C}_{1,1} & \mathbf{C}_{1,2} & \mathbf{C}_{1,3} & \mathbf{D}f - \mathbf{K} - \mathbf{I}_n & \mathbf{K} & & & \mathbf{O} \\ \mathbf{0}_{n\times n} & \mathbf{0}_{n\times n} & \mathbf{0}_{n\times d} & \mathbf{I}_n & -\mathbf{I}_n & & & \\ \vdots & \vdots & \vdots & & & \ddots & & \\ \mathbf{C}_{2d-1,1} & \mathbf{C}_{2d-1,2} & \mathbf{C}_{2d-1,3} & & & & \mathbf{D}f - \mathbf{K} - \mathbf{I}_n & \mathbf{K} \\ \mathbf{0}_{n\times n} & \mathbf{0}_{n\times n} & \mathbf{0}_{n\times d} & \mathbf{O} & & & \mathbf{I}_n & -\mathbf{I}_n \end{vmatrix}.$$

By applying elementary column operations to $\mathbf{D}\boldsymbol{F} - \mathbf{I}_{2n+d+2nd}$, namely, adding the rightmost column block to the second rightmost column block, we obtain a block-upper-triangular matrix with two diagonal blocks, the lower right diagonal block of which is $-\mathbf{I}_n$, as follows:

$$|\mathbf{D}\boldsymbol{F} - \mathbf{I}_{2n+d+2nd}| = \begin{vmatrix} \mathbf{D}f - \mathbf{K} - \mathbf{I}_n & \mathbf{K} & \mathbf{A}_{1,3} & \mathbf{0}_{n\times n} & \mathbf{0}_{n\times n} & \dots & \mathbf{0}_{n\times n} & \mathbf{0}_{n\times n} \\ \mathbf{I}_n & -\mathbf{I}_n & \mathbf{0}_{n\times d} & \mathbf{0}_{n\times n} & \mathbf{0}_{n\times n} & \dots & \mathbf{0}_{n\times n} & \mathbf{0}_{n\times n} \\ \mathbf{A}_{3,1} & \mathbf{A}_{3,2} & \mathbf{0}_{d\times d} & \mathbf{B}_{3,1} & \mathbf{B}_{3,2} & \dots & \mathbf{0}_{d\times n} & \mathbf{B}_{3,2d} \\ \mathbf{C}_{1,1} & \mathbf{C}_{1,2} & \mathbf{C}_{1,3} & \mathbf{D}f - \mathbf{K} - \mathbf{I}_n & \mathbf{K} & & & \mathbf{O} \\ \mathbf{0}_{n\times n} & \mathbf{0}_{n\times n} & \mathbf{0}_{n\times d} & \mathbf{I}_n & -\mathbf{I}_n & & & \\ \vdots & \vdots & \vdots & & & \ddots & & \\ \mathbf{C}_{2d-1,1} & \mathbf{C}_{2d-1,2} & \mathbf{C}_{2d-1,3} & & & & \mathbf{D}f - \mathbf{I}_n & \mathbf{K} \\ \mathbf{0}_{n\times n} & \mathbf{0}_{n\times n} & \mathbf{0}_{n\times d} & \mathbf{O} & & & \mathbf{0}_{n\times n} & -\mathbf{I}_n \end{vmatrix}.$$

Note that $\mathbf{B}_{3,2d-1} + \mathbf{B}_{3,2d} = \mathbf{0}_{d\times n}$ (see Appendix A). We see that the upper left diagonal block is a block-lower-triangular matrix, the lower right diagonal block of which is $\mathbf{D}\boldsymbol{f} - \mathbf{I}_n$. Because the determinant of a block-triangular matrix is the product of the determinants of diagonal blocks, we have

$$|\mathbf{D}\boldsymbol{F} - \mathbf{I}_{2n+d+2nd}| = |\mathbf{A} - \mathbf{I}_{2n+d}|(|\mathbf{D}\boldsymbol{f} - \mathbf{I}_n||-\mathbf{I}_n|)^d$$

by repeatedly applying the above procedure to the remaining upper left diagonal block of the block-lower-triangular matrix. By applying elementary row and column operations to $\mathbf{A} - \mathbf{I}_{2n+d}$, it is not difficult to see $|\mathbf{A} - \mathbf{I}_{2n+d}| = 0$. Therefore, $|\mathbf{D}\boldsymbol{F} - \mathbf{I}_{2n+d+2nd}| = 0$, and we obtain the fact.

APPENDIX C: DERIVATION OF THE FIXED POINTS OF ADAPTIVE DFC SYSTEMS

We can derive the form of the fixed points of Eq. (4) by solving the equation $\tilde{\mathbf{x}} = \boldsymbol{F}(\tilde{\mathbf{x}})$ (see Appendix A for explanation of the symbols). Since $\boldsymbol{F}_{\mathbf{y}}$ is the n-dimensional identity map, we have $\mathbf{y} = \mathbf{x}$. Then, the second term of $\boldsymbol{F}_{\mathbf{x}}$ vanishes, and we have $\mathbf{x} = \mathbf{y} = \mathbf{x}_*$. Similarly, the second term of $\boldsymbol{F}_{\boldsymbol{\kappa}}$ vanishes, and $\boldsymbol{\kappa}$ becomes an arbitrary d-dimensional constant vector. Since $\boldsymbol{F}_{\mathbf{w}_l}$ is also the n-dimensional identity map, we have $\mathbf{w}_l = \mathbf{v}_l$ for $l = 1,2,\ldots,d$. Then, the second and third terms of $\boldsymbol{F}_{\mathbf{v}_l}$ vanish, and we have $\mathbf{v}_l = \mathbf{D}\boldsymbol{f}(\mathbf{x}_*)\mathbf{v}_l$. If $\mathbf{D}\boldsymbol{f}(\mathbf{x}_*)$ has eigenvalue unity, then we have $\mathbf{v}_l = \mathbf{w}_l = \mathbf{z}_l$ for $l = 1,2,\ldots,d$. Otherwise, $\mathbf{v}_l = \mathbf{w}_l = \mathbf{0}$.

APPENDIX D: PROOF OF FACT 3

In this appendix, a proof of Fact 3 is presented. Let $\tilde{\mathbf{x}}_*$ be a fixed point of Eq. (4), satisfying $\tilde{\mathbf{x}}_* = \boldsymbol{F}(\tilde{\mathbf{x}}_*)$ (see Appendix A for explanation of the symbols). From Fact 2, the $\mathbf{x}$ and $\mathbf{y}$ components of $\tilde{\mathbf{x}}_*$ coincide, that is, $\mathbf{x} = \mathbf{y} = \mathbf{x}_*$. Then, $\mathbf{A}_{1,3}$ and $\mathbf{B}_{3,i}$ $(i = 1,2,\ldots,2d)$ become zero matrices at $\tilde{\mathbf{x}}_*$ (see Appendix A), and $\mathbf{D}\boldsymbol{F}(\tilde{\mathbf{x}}_*)$ becomes a block-lower-triangular matrix from Eq. (A5). Because the determinant of a block-triangular matrix is the product of the determinants of diagonal blocks, the characteristic polynomial of $\mathbf{D}\boldsymbol{F}(\tilde{\mathbf{x}}_*)$ is given by

$$|\lambda\mathbf{I}_{2n+d+2nd} - \mathbf{D}\boldsymbol{F}(\tilde{\mathbf{x}}_*)| = (\lambda-1)^d \left|\lambda\mathbf{I}_{2n} - \begin{pmatrix} \mathbf{D}\boldsymbol{f}(\mathbf{x}_*) - \mathbf{K} & \mathbf{K} \\ \mathbf{I}_n & \mathbf{0}_{n\times n}\end{pmatrix}\right|^{d+1}.$$

Since

$$\Phi(\lambda) = \left|\lambda\mathbf{I}_{2n} - \begin{pmatrix} \mathbf{D}\boldsymbol{f}(\mathbf{x}_*) - \mathbf{K} & \mathbf{K} \\ \mathbf{I}_n & \mathbf{0}_{n\times n}\end{pmatrix}\right|,$$

we obtain the fact.

[1] J. F. Kolen and J. B. Pollack, Complex Syst. **4**, 269 (1990).
[2] T. Hondou and Y. Sawada, Prog. Theor. Phys. **91**, 397 (1994).
[3] H. Nakajima and Y. Ueda, Phys. D (Amsterdam) **99**, 35 (1996).
[4] A. Saito, M. Taiji, and T. Ikegami, Phys. Rev. Lett. **93**, 168101 (2004).
[5] K. Pyragas, Phys. Lett. A **170**, 421 (1992).
[6] E. Ott, C. Grebogi, and J. A. Yorke, Phys. Rev. Lett. **64**, 1196 (1990).
[7] K. Yamasue and T. Hikihara, Phys. Rev. E **69**, 056209 (2004).
[8] W. Just, H. Benner, and C. von Loewenich, Phys. D (Amsterdam) **199**, 33 (2004).
[9] G. Chen and X. Dong, *From Chaos to Order* (World Scientific, Singapore, 1998).
[10] *Handbook of Chaos Control*, 2nd ed., edited by E. Schöll and H. G. Schuster (Wiley-VCH, Weinheim, 2008).
[11] K. Pyragas, Philos. Trans. R. Soc. A **364**, 2309 (2006).
[12] S. Bielawski, D. Derozier, and P. Glorieux, Phys. Rev. A **47**, R2492 (1993).
[13] T. Ushio, IEEE Trans. Circuits Syst. I **43**, 815 (1996).
[14] K. Konishi and H. Kokame, Phys. Lett. A **248**, 359 (1998).
[15] H. Nakajima, H. Ito, and Y. Ueda, IEICE Trans. Fundam. Electron. Commun. Comput. Sci. **E80-A**, 1554 (1997).
[16] R. J. Williams and D. Zipser, Neural Comput. **1**, 270 (1989).
[17] K. Doya, in *The Handbook of Brain Theory and Neural Networks*, 2nd ed., edited by M. Arbib (MIT, Cambridge, MA, 2002).
[18] H. G. Schuster and W. Just, *Deterministic Chaos*, 4th ed. (Wiley-VCH, Weinheim, 2005).
[19] E. Ott, *Chaos in Dynamical Systems*, 2nd ed. (Cambridge University, Cambridge, UK, 2002).
[20] K. Ogata, *Discrete-Time Control Systems* (Prentice Hall, Englewood Cliffs, NJ, 1995).
[21] P. Manneville, J. Phys. (Paris) **41**, 1235 (1980).
[22] K. Chen, P. Bak, and M. H. Jensen, Phys. Lett. A **149**, 207 (1990).
[23] J. F. Heagy, N. Platt, and S. M. Hammel, Phys. Rev. E **49**, 1140 (1994).
[24] J. L. Cabrera and J. G. Milton, Phys. Rev. Lett. **89**, 158702 (2002).